A Novel Statistical Approach to Obtain the Best Visibility Slice in MRI Sequence of Brain Tumors

Hassan Al-Yassin[1] 🆔 ✉, *Mohammed A. Fadhel *[2]* 🆔 ✉, *Omran Al-Shamma[1]* 🆔 ✉

[1]Department of Quality Assurance, College, University of Information Technology and Communications, Baghdad, Iraq.

[2]Department of Computer Information Systems, College of Computer Science and Information Technology, University of Sumer, Thi Qar, Iraq.

3Department of Scientific Affairs, College, University of Information Technology and Communications, Baghdad, Iraq.

*Corresponding Author.

Abstract

Early diagnosis of brain tumor enhances the possibility of patients being cured. With the progress of the use of artificial intelligence in the medical field, the detection of brain tumors has become one of the researchers' interests. Obtaining which slice in the MRI sequence gives the best visibility of the tumor is still a challenge. This paper introduced a novel statistical approach to extracting the tumor from the patient's MRI scan (sequence). Initially, the probability mass function (PMF) was computed for each image in the sequence. Then, the Kullback-Leibler divergence technique was applied to determine the tumor image(s) that diverged from the respective healthy ones. The best tumor visibility slice was determined using the root mean square error metric. In addition, a clustering approach was applied to segment the tumor images. The vector quantization (VQ) method was utilized for grouping the images into 16 different clusters, while a reverse VQ technique was employed to produce two-tone images. Finally, a 2D Teager operator was used to detect the edges for tumor demarcation. A private dataset of twenty MRI scans (sequences) was used for testing and evaluating the system.

Keywords: Brain tumor, Kullback-Leibler divergence, MRI images, Probability mass function, Tumor detection.

Introduction

Tumor diagnosis at early stages enhances the probability of curing patients. Brain tumors are of two major types: non-cancerous (so-called benign), and cancerous (so-called malignant)[1]. In surgical processes, assigning tumor boundaries is very sensitive and must be identified accurately, as well as the border between the normal and abnormal tissues [1]. Magnetic resonance imaging (MRI) provides a reliable source of information for high-quality medical imaging. Thus, it has become widely used. MRI is a gold standard for brain tumor diagnosis [2]. Detailed images of the body, in any direction, are provided by MRI, with rich information about the human soft-tissue anatomy [3]. For detecting tumor boundaries, it is required to partition the medical images into different segments based on preselected features. Image segmentation has two approaches, either discontinuities or similarities. Pixel intensity is the most used feature.

The "Customized Segment Anything Model" is a prominent scholarly contribution in the field of

medical image segmentation, catering to specific segmentation requirements [4]. The authors Saha et al. developed a novel approach called DEMARCATE (DEnsity-based Magnetic Resonance image Clustering) for the purpose of analyzing tumor heterogeneity based on images [5]. The whole of the tumor voxel space is used to get the comprehensive tumor heterogeneity density profiles (THDPs), which are then analyzed [6]. Sikandar and Mahum [6] proposed a technique to address the problem of oversampling in MRI/CT scan image pre-processing. Their approach involves applying Sobel edge operators to the images before using the watershed segmentation algorithm for tumor identification [7]. Amin and et al. used a fuzzy clustering-based approach [8] to examine and investigate the intricate composition of the brain in MRI images. They developed a methodology for the detection of brain tumors in MRI images by using statistical data to calculate the disparity between distinct brain regions. In order to partition the tumor into distinct regions and calculate its surface area, the researchers used a fuzzy transform and morphological procedure. In reference [9], researchers used the Linde Buzo Gray Algorithm (LBG), a vector quantization technique, to categorize fingerprint images. The researchers achieved an accuracy rate of 80% by using a codebook with a size of 4 and a window size of 8×8. Dhole and Dixit [10] presented a review article for the detection and analysis of brain tumors. In their technique, the MRI images are divided into equal quadrants, and afterwards, denoise and contrast filters are used to increase the quality of the images. In addition to using a Canny edge detection approach, regional property grouping and maximal transformation were also used in order to locate the tumor [11]. The vector quantization (VQ) technique was developed by Taylor et al. with the aim of discerning and differentiating cancers in magnetic resonance imaging (MRI) images. It has been shown that VQ exhibits superior performance in comparison to the grey-level co-occurrence matrices technique. The latter method is characterized by a long processing time and tends to generate over-segmentation as a result of the watershed algorithm [12, 13].

The main objective of this research was to overcome the challenge of identifying the most effective MRI slice for optimal brain tumor visibility. The researchers utilized a novel statistical strategy to improve tumor information extraction from patient MRI data. The recommended strategy for locating the slice with the best visibility is calculating the PMF for each image in the MRI sequence. Simultaneously, the tumor's boundary location was determined through image retrieval analysis. Tumor extraction was achieved using a vector quantization method with a codebook of size 16, along with a reverse quantization technique to generate a two-tone image. To delineate tumor boundaries, a 2D Teager power operator served as an edge detector. Notably, there is currently no existing literature on a method or approach for obtaining the optimal visibility slice from an MRI scan. Therefore, this innovative approach not only improves tumor detection but also facilitates accurate tumor classification. The potential significance of this concept lies in its ability to advance medical imaging methodologies, with the potential for improved patient care and outcomes, especially in the field of neuro-oncology.

Methods

Several methods were utilized in this work, including probability mass function, vector quantization technique, and Teager power operator.

A. Probability Mass Function (PMF)

One of the essential concepts in statistics and probability theory is the probability mass function (PMF). For a discrete random variable, it expresses the probability distribution. More specifically, for a discrete random variable, each likely outcome is assigned probabilities by the PMF. For instance, when flipping a coin many times, the possible outcomes are the number of heads gotten. However, PMF is widely used in different fields like economics, biology, physics, and engineering. It is a fundamental tool for random variables to calculate the predictable variances, values, and other statistical metrics. Furthermore, it concludes and makes predictions for populations in statistical modeling and hypothesis testing [8, 14].

In mathematics, as outlined in Eq. 1, let A be a discrete random variable, so its range R_A is a countable set. In particular:

$$R_A = \{a_1, a_2, a_3, \dots\} \qquad 1$$

Note that a_1, a_2, a_3, … are possible values of A. In addition, if $A = a_i$, then the event $X = \{A=a_i\}$ is denoted as an outcome set t in the sample space T, and it can be written as defined in Eq. 2:

$$X = \{t \in T \mid A(t) = a_i\} \qquad 2$$

Thus, the PMF is formally shown the probabilities of events $\{A = a_i\}$ in its definition:

$$P_A(a_i) = P(A = a_i), \qquad \text{for } i = 1, 2, 3, … \qquad 3$$

Eq. 3 is known as the PMF of A. Thus, for a given random variable, the PMF gives the probabilities of achievable values. Hence, it is a probability measure.

Consequently, the PMF has two main properties. First, it is non-negative measure. The summation of probabilities is equal to one around the whole achievable values.

In contrast, the probability density function (PDF) is used rather than PMF for a continuous random variable. The PDF assigns probabilities for periods of values owing to the continuous nature of the variable, while PMF assigns probabilities for specific values.

B. Kullback-Leibler

The discrepancy between two probability distributions is measured by the Kullback-Leibler (KL) divergence, which is also called relative entropy. It is an idea found in statistics and information theory. It was developed in the 1950s by Solomon Kullback and Richard Leibler as a method of quantifying the difference between two probability distributions. Statistics, machine learning, data analytics, and information theory are just a few of the disciplines where KL divergence has applications [15,16].

In mathematics, as expressed in Eq. 4, the KL divergence from P to Q is defined as follows given two discrete probability distributions P and Q over the same event space.

$$D_{KL}(P||Q) = \sum_{i \in L} P(i) \log \frac{P(i)}{Q(i)} \qquad 4$$

Where p(i) and q(i) are the probability mass functions of P and Q, while L is the intensity level. All images are examined to obtain the suitable distance metric for distinguishing between tumor and

healthy images. As stated in the findings section, it has been demonstrated that this kind of distance metric is significantly superior to the RMSE.

C. Vector Quantisation Technique (VQ)

Vector quantization of image intensity is available in several applications that differ in cluster formation [10, 12, 13]. The VQ technique formulates the next two clusters by multiplying the average intensity of the image by 1.01 and 0.09, respectively, to produce new two-intensity clusters. The pixels of the image are distributed between these two new clusters according to the minimum Euclidean distance between the pixel intensity and the intensities of one of the two new clusters. Then, a new average is computed for each new cluster according to the intensities of each pixel. The pixels of the image are redistributed between the two new clusters using their new averages. This procedure is repeated until the currently distributed pixels in each new cluster are similar to the distribution of the previous iteration or the number of iterations reaches 100. Each one of the resultant two clusters is then separated into two new clusters by multiplying the average of each cluster by 1.01 and 0.09, respectively, as before. So now the pixels of the image are distributed between four clusters of intensities. This procedure is continued until 16 intensity levels are generated.

D. Teager Power Operator

Teager described the nonlinear production of speech in his article 'Evidence for Nonlinear Sound Production Mechanisms in the Vocal Tract' in 1990. At the same time, Kaiser [17] introduced a technique for computing the signal energy and named it as 'Teager Energy Algorithm'.

Eq. 5 provides the definition of the continuous Teager energy operator:

$$\Phi(x(t)) = \dot{x}^2(t) - x(t)\ddot{x}(t) \qquad 5$$

where $\dot{x}$ means the first derivative of x, and $\ddot{x}$ means the second derivative, and as is defined in Eq. 6:

$$\Phi[x[n]] = x2[n] - x[n-1]x[n+1] \qquad 6$$

The 2D version of the discrete Teager energy operator is defined along the diagonal directions [18, 19] as articulated in Eqs. 7 and 8:

$$\Phi d[m,n] = 2x2[m,n] - x[m-1,n+1]x[m+1,n-1] - x[m-1,n-1]x[m+1,n+1] \qquad 7$$

Also, along the cross pixels, it is:

$$\Phi p[m,n]=2x2[m,n]-x[m,n+1]x[m,n-1]-x[m-1,n]x[m+1,n] \qquad 8$$

Where $\Phi d[m,n]$ and $\Phi p[m,n]$ are diagonal and cross Teager operators using the diagonal and cross pixels of the current pixel (m,n), and x[m,n] is the intensity of the pixel (m,n). Then the maximum of these two operators (diagonal, cross) is used to represent the edge. The local activity of the image is better reflected by the 2D Teager operator than the classical edges detection operator [18, 20]. The resulting image would highlight the boundaries of separate structures inside the MRI scan [21], making it easier for medical practitioners to identify and analyze anatomical demarcations.

It is vital to remember that in order to get the best results, the approach may need additional operations such as noise reduction, parameter adjustment, and post-processing. The Teager Power Operator combined with gradient information improves the perceptiveness of edge recognition in magnetic resonance imaging (MRI) images.

Proposed System

The proposed aims to detect the tumor boundaries accurately using a novel statistical approach. Its flow-work consists of five principal stages, as illustrated in Fig. 1.

1. Input Images.
2. Image Pre-processing.
3. Calculating the PMF to detect the tumor in each image in MRI sequence.
4. Applying vector quantization of codebook of size 16 technique and forming a two-tone image using proposed reverse quantization algorithm.
5. Applying 2-D Teager operator for edge detection of the tumors.

In the first stage, the input image sequence is pre-processed using a maiden filter of size 3 to remove noises. This filter is a part of the MATLAB-R2023a image processing toolbox. The second stage includes a PMF function. It is computed for each processed sequence to detect the tumor in each image. Since the digital image is defined as a two-dimensional function x(m,n), representing the digital scale intensity of the pixel at the spatial discrete coordinates m and n. This function x(m,n) is produced by sampling and quantizing the analog

image's coordinates and amplitude [14]. A digital greyscale of intensity is used, so for 8-bit representation, there will be 256 intensity levels (L), and the function x(m,n) is randomly assigned one of these levels. Therefore, this function is considered a random variable, and the PMF can be computed by dividing the image's histogram by all pixels in the image [15]. The histogram is the number of times intensity level r_k appears in the image is defined in Eq. 9:

$$H(r_k) = n_k \qquad \text{for k=1,2,…,256} \qquad 9$$

where n_k is the number of times intensity level r_k appears. Thus, the PMF is defined in Eq. 10:

$$P(r_k) = \frac{n_k}{NM} \qquad \text{for k=1,2,…,256} \qquad 10$$

Moreover, N and M are the total number of columns and rows of the image, respectively.

Each image of the MRI brain scans from the sequences of both healthy and patient is applied to the PMF calculation procedure. The root means square error (RMSE) between the PMF of the healthy and the patient image is then calculated. Now, the proposed reversed VQ is used to generate a binary image. Finally, the 2D Teager operator is employed to detect the tumor edges.

In addition, the root means square error technique (RMSE) is applied to measure the difference between the resultant PMFs of the patient and the healthy. The images that achieved high values of RMSE are classified as abnormal. The Kullback-Leibler divergence is also applied in this stage to enhance the detecting accuracy of images with brain tumors. Next, in the third stage, the abnormal images are quantized into a 16-level image using the VQ method with a codebook of size 16. Note that several VQ methods were developed for cluster formation [10]; the selected method in this work will discussed later. The fourth stage, which is called reverse quantization (or dequantization), involves converting the 16-level images into two-tone ones because it is difficult to detect the tumor boundary from the resultant 16-level quantized image. More specifically, this stage is performed in two steps. In the first step, a four-level mode is composed by examining each pixel level, starting with the mid-range point. If the pixel level is greater than the mid-range point, it is then compared with the three-quarter value of the range. As a result of comparison, a higher output value is categorized as level four; otherwise, it is level three. In contrast, if the pixel level is less than the mid-range point, then it is compared with the quarter value of the range. On

account of comparison, a lower value is categorized as level two; otherwise, it is level one. In the second step, the resultant four-level images are converted into two-tone by examining each pixel with level two. If it is greater than two, it is categorized as level two; otherwise, it is level one. Consequently, the image background is represented by pixels of level one, while the pixels of the tumor will be of level two. The last stage (stage five) includes applying the 2D Teager power operator on the resultant two-tone images to detect the tumor edge. This operator emphasizes sudden shifts in intensity. This method computes energy using adjacent pixels in both dimensions, thus emphasizing the potential boundaries of tumors. Employing this operator enhances the clarity of tumor edges, and subsequent steps like thresholding can extract these enhanced edges to precisely detect tumors. The efficacy of this approach relies on factors like image quality, tumor attributes, and parameter selections.

Figure 1. The flow work of the statistical approach.

Results and Discussion

The results of this work highlight the potential gains and changes that may be made in the area of medical imaging, particularly in tumor diagnosis and assessment. The brain dataset used in this study was gathered from Baghdad Teaching Hospital/Medical City in Baghdad, Iraq. It comprised MRI sequences from 20 individuals, including both patients and healthy. Each sequence consisted of 18 MRI images, representing a complete brain scan, as displayed in Figs. 2 and 3. The proposed technique didn't yield success unless the original sorting of MRI images was considered. Therefore, proper sorting was crucial for examining the largest brain tumor in each slice.
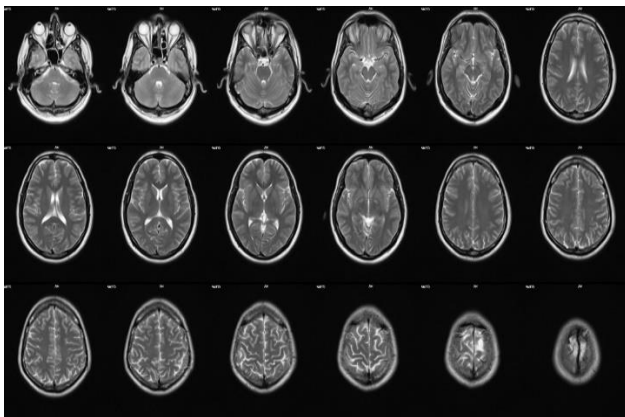
In the initial phase, a filter was applied to the input series of images to eliminate any noise. Then, the PMF was calculated for each processed image in the sequence for both the patient and the healthy individual. The RMSE method was used to determine the difference between the resulting PMFs of the patient and the healthy person for each image in the sequence. High RMSE values indicate that the patient's images are abnormal.
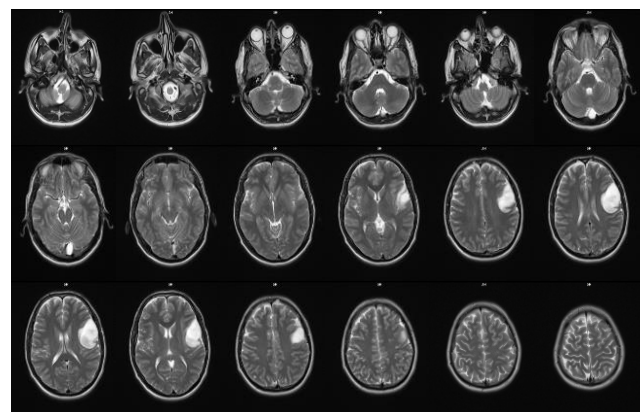

Figure 3. Slice of MRI for a patient's brain.

As illustrated in Figs. 5 and 6, the PMF curves are similar, but there is a tiny difference in the second peak. It means that the PMF curve is directly affected by the intensity of the tumor. For normal cases, the

Figure 2. MRI image sequence for healthy (normal) brain.

second max peak occurred at 0.33 on the x-axis, while the tumor brain was at 0.29.
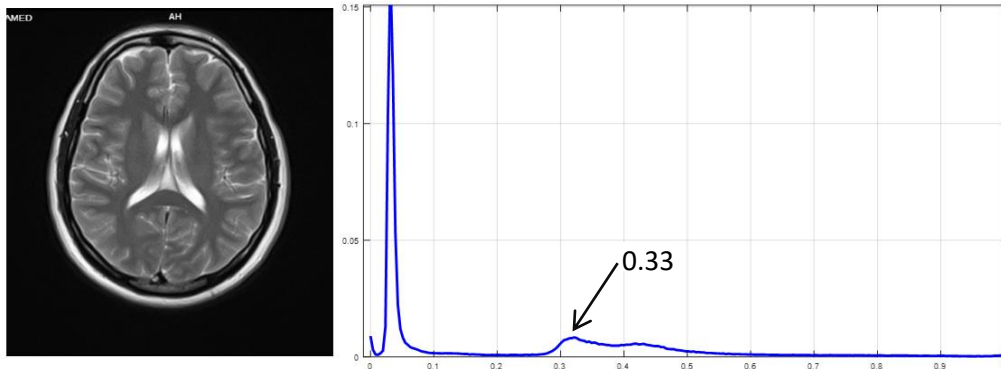

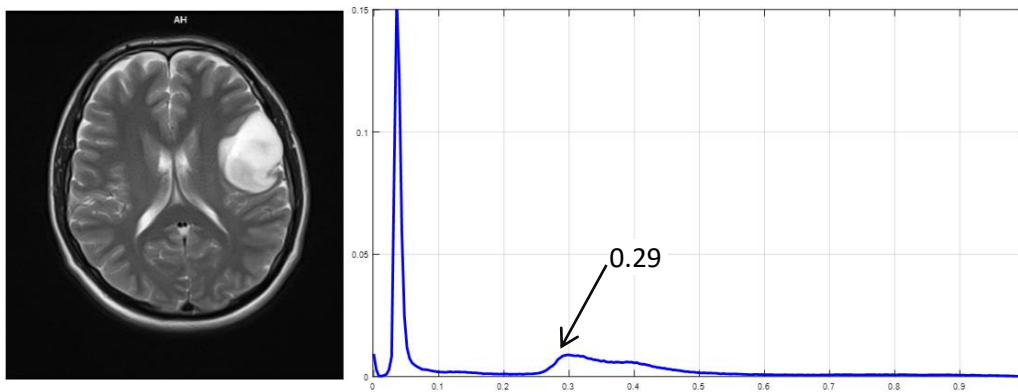**Figure 5. PMF for one slice of MRI (normal).**

Figure 6. PMF for one slice of MRI (tumor).

As mentioned earlier, intensity plays a leading role in image processing techniques. The RMSE for intensity values was applied to 18 MRI slices between normal and patient slices Fig. 7.
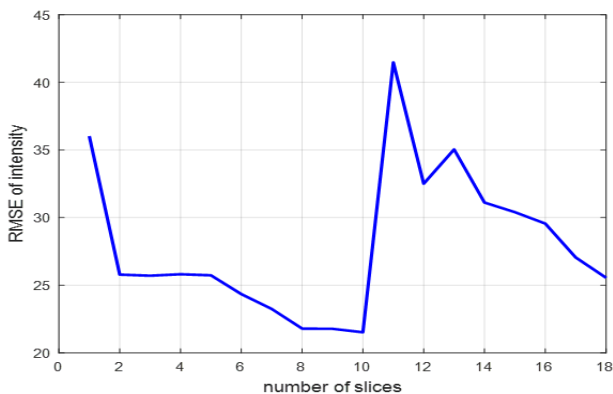

Figure 7. RMSE for intensity values between normal and patient slices.

In addition, the RMSE for the computed PMF values was calculated for each corresponding image in the sequence of the healthy and patient. Fig. 8 illustrates the RMSE between the images in the two mentioned sequences. The maximum peak seen at slice number

13 means that the tumor's biggest area appears in that slice of the patient's brain. This result is not extremely identical to the images shown in Fig. 3, where the tumor started from slice number 8 to slice number 13, and no threshold can be chosen to distinguish between the healthy and the one that contained the tumor.
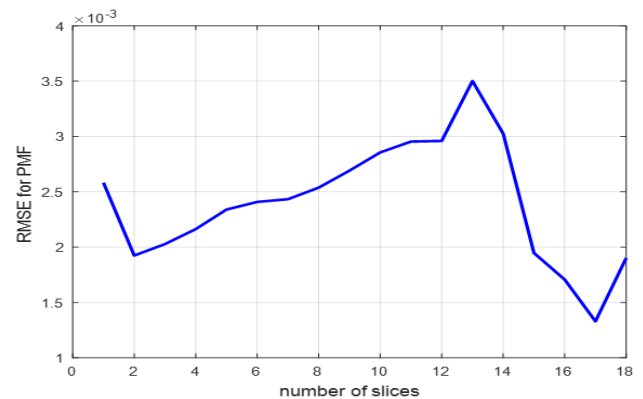

Figure 8. RMSE for PMF values between normal and patient slices.

The Kullback-Leibler divergence was applied to overcome the previous drawback of the RMSE and

to enhance the accuracy of detecting images with a brain tumor. As clarified in Fig. 9, the plotted curve is slightly different from the Fig. 8 curve due to the logarithm function in Eq. 3, which works to enlarge the fine details in the curves. The heights of the various peaks indicate the stages of the appearance of the tumor in the MRI slices. Thus, it is clear from Fig. 9 that a threshold can be specified to distinguish the images with tumors from those without them.
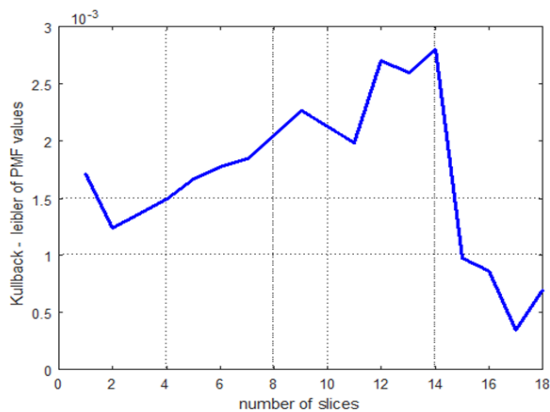

Figure 9. Kullback-Leibler divergence of PMF values between normal and patient slices.

Therefore, this work elucidates the efficient application of Probability Mass Function (PMF) attributes to assist in the extraction of tumors in various medical image slices. The flexibility and adaptability of statistical criteria for tumor identification and evaluation in medical imaging analysis are highlighted by their effective implementation into different image segments. Moreover, the examination of the utilization of Root Mean Square Error (RMSE) and Kullback-Leibler metrics to distinguish disparities between magnetic resonance imaging (MRI) scans of individuals with and without brain-related disorders demonstrates a quantitative methodology for detecting pathological alterations. The examination of these metrics in the paper underscores the heightened precision of Kullback-Leibler as a result of its logarithmic characteristics, which provide a more comprehensive depiction of the complexity inherent in images.

Then the marked images of the patient were quantized into 16-level images using the vector quantization procedure of the codebook of size 16. The boundary of the tumor is difficult to detect from the resultant quantized image, as displayed in Fig. 10 (the second image of the second row). It is clear from this figure that the first binary image produced by the VQ method cannot be used to identify the tumor.

Thus, a proposed algorithm was applied to return from this 16-level image to one of the two-tone images (de-quantization), which can separate the tumor from the background of the image, as shown in Fig. 11 (the second image of the second row). The resultant composed two-tone image was applied to a 2D Teager power operator to detect the edge of the tumor (first image of the second row in Fig. 11).

The usefulness of 16-level quantization and de-quantization approach in boosting tumor visibility by clearly distinguishing tumor areas from the surrounding backdrop in medical images has been proven in the research. This discovery exhibits potential as a viable and realistic solution for enhancing tumor distinction in the context of medical imaging applications. The significant results have crucial implications, not only in improving the diagnostic capabilities of medical imaging but also in guiding future research endeavors that may include the integration of sophisticated quantization methods and machine learning approaches to further increase tumor identification and assessment.
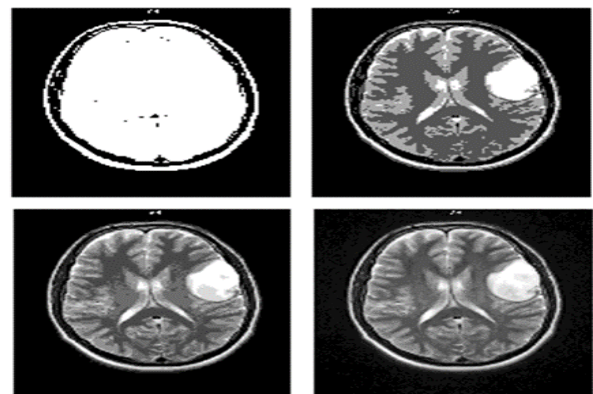

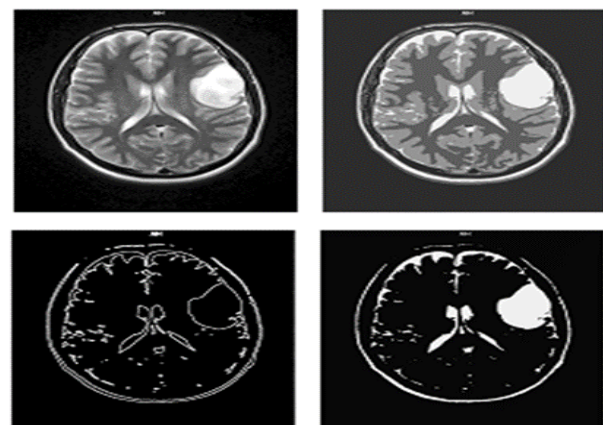**Figure 10. Vector quantization procedure of 16-level image.**

Figure 11. The de-quantization procedure and the edge-detected image.

Conclusion

In summary, this research addressed the persistent challenge of determining the optimal visibility slice in MRI scans, offering a significant contribution to the field of medical imaging. The study introduced innovative perspectives on diverse approaches and metrics, providing transformative insights into tumor diagnosis and evaluation. The applied statistical approach, which utilized the probability mass function with the root mean square error metric, proved effective in identifying the slice with optimal tumor visibility. Furthermore, the employment of the Kullback-Leibler divergence technique enhanced the extraction of tumor images that significantly diverged from healthy counterparts.

The incorporation of a statistical approaches, featuring vector quantization and reverse vector quantization techniques, showcased the potential for tumor segmentation through the generation of two-tone images. Notably, the accurate detection of tumor boundaries using the 2D Teager operator represented a notable success in this research. The utilization of a private dataset in the absence of online MRI sequence availability demonstrated adaptability and resourcefulness.

This paper suggested a promising avenue for future research by proposing the integration of machine learning techniques. This envisioned enhancement aimed to further boost diagnostic accuracy, particularly in fine-tuning the selection of optimal MRI slices and refining tumor identification methods. The research stood as a testament to the evolving landscape of technology and analytical methodologies in medical imaging, laying the groundwork for continued exploration and refinement in the dynamic field of neuro-oncology.

Authors' Declaration

- Conflicts of Interest: None.
- We hereby confirm that all the Figures and Tables in the manuscript are ours. Furthermore, any Figures and images, that are not ours, have been included with the necessary permission for re-publication, which is attached to the manuscript.

- Authors sign on ethical consideration's approval.
- No animal studies are present in the manuscript.
- Ethical Clearance: The project was approved by the local ethical committee at University of Sumer.

Authors' Contribution Statement

Idea development by H. A. Y. and M. A. F. methodology by M. A. F. and O. A. S. software design and implementation, as well as initial draft preparation, by H. A. Y. and M. A. F., and O. A. S.

review and editing contributions from all authors. All authors have reviewed and approved the final manuscript for publication.

References

1. Thiyagarajan P, Padmanaban S, Thiruvenkadam K, Karuppanagounder S. Advancements of MRI-Based Brain Tumor Segmentation from Traditional to Recent Trends. Curr Med Imaging Rev. 2022. 18; 18(12): 1261 - 1275. https://doi.org/10.2174/15734056176662112151119337 .
2. Rehman MU, Ryu J, Nizami IF, Chong KT. RAAGR2-Net: A brain tumor segmentation network using parallel processing of multiple spatial frames. Comput Biol Med. 2023; 152:106426. https://doi.org/10.1016/j.compbiomed.2022.106426 .
3. Al-Ani NQ, Al-Shamma O. A review on detecting brain tumors using deep learning and magnetic resonance images. Int J Electr Comput Eng. 2023; 13: 4582-4593. http://doi.org/10.11591/ijece.v13i4.pp4582-4593 .
4. Zhang K, Liu D. Customized Segment Anything Model for Medical Image Segmentation. arXiv.org. 2023. https://doi.org/10.48550/arXiv.2304.13785 .
5. Saha A, Banerjee S, Kurtek S, Narang S, Joon Sang Lee, Rao G, et al. demarcate: Density-based magnetic resonance image clustering for assessing tumor heterogeneity in cancer. Neuro Imag: Clinic. 2016; 12: 132–43. https://doi.org/10.1016/j.nicl.2016.05.012 .
6. Sikandar S, Mahum R, Alsalman A. A Novel Hybrid Approach for a Content-Based Image Retrieval Using Feature Fusion. App Sci. 2023; 13(7): 4581. https://doi.org/10.3390/app13074581 .

7. El-Sherbiny B, Nabil N, El-Naby SH, Emad Y, Ayman N, Mohiy T, et al. BLB (Brain/Lung cancer detection and segmentation and Breast Dense calculation). 1st International Workshop on Deep and Representation Learning (IWDRL). IEEE Xplore. 2018: 41–7. https://doi.org/10.1109/IWDRL.2018.8358213 .

8. Amin J, Sharif M, Raza M, Saba T, Anjum MA. Brain tumor detection using statistical and machine learning method. Comput. Methods Programs Biomed. 2019; 177: 69–79. https://doi.org/10.1016/j.cmpb.2019.05.015 .

9. Bakshi A, Gupta A, Tanwar S, Sharma G, Bokoro PN, Alqahtani F, et al. Performance Augmentation of Cuckoo Search Optimization Technique Using Vector Quantization in Image Compression. Math. 2023; 11: 2364. https://doi.org/10.3390/math11102364 .

10. Dhole NV, Dixit VV. Review of brain tumor detection from MRI images with hybrid approaches. Multimed. Tools Appl. 2022; 81:10189–10220. https://doi.org/10.1007/s11042-022-12162-1 .

11. Soomro TA, Zheng L, Afifi AJ, Ali A, Soomro S, Yin M, et al. Image Segmentation for MR Brain Tumor Detection Using Machine Learning: A Review. IEEE Rev Biomed Eng. 2022 ;16: 1–21. https://doi.org/10.1109/RBME.2022.3185292 .

12. Hasan AM, Qasim AF, Jalab HA, Ibrahim RW. Breast cancer MRI classification based on fractional entropy image enhancement and deep feature extraction. Baghdad Sci J. 2023; 20 (1): 0221-0221. https://doi.org/10.21123/bsj.2022.6782 .

13. Laith Alzubaidi, Bai J, Aiman Al-Sabaawi, Santamaría J, Albahri AS, Bashar, et al. A survey on deep learning tools dealing with data scarcity: definitions, challenges, solutions, tips, and applications. J Big Data. 2023; 10: 46. https://doi.org/10.1186/s40537-023-00727-2 .

14. Gonzalez RC, Woods RE. Digital image processing. New York, Ny: Pearson; 2018. https://doi.org/10.4236/ijg.2014.55050 .

15. Wang C, Shen HW. Information Theory in Scientific Visualization. Entropy. 2011; 13: 254–73. http://dx.doi.org/10.3390/e13010254

16. Teager HM, Teager SM. Evidence for Nonlinear Sound Production Mechanisms in the Vocal Tract. Speech Production and Speech Modelling. 1990; 241–61. http://dx.doi.org/10.1007/978-94-009-2037-8_10.

17. Kumar BR, Joseph DK, Sreenivas TV. Teager energy-based blood cell segmentation. In: 14th International Conference on Digital Signal Processing Proceedings.; Santorini, Greece. 2002; 2: 619-622. https://doi.org/10.1109/ICDSP.2002.1028167 .

18. Abdel-Ouahab Boudraa, El. Image contrast enhancement based on 2D Teager-Kaiser operator. 15th IEEE International Conference on Image Processing. 2008. https://doi.org/10.1109/ICIP.2008.4712471 .

19. Zhang X, Qin Y, Li Y, Feng X, Li B, Hu X, et al. A GPR 2D Teager-Kaiser energy operator based on the multivariate variational mode decomposition. Remot Sens Lett. 2022; 14: 30–8. https://doi.org/10.3390/rs14194805 .

20. Yaseen BT, Kurnaz S, Ahmed SR. Detecting and Classifying Drug Interaction using Data mining Techniques. In: 2022 International Symposium on Multidisciplinary Studies and Innovative Technologies (ISMSIT); Ankara, Turkey; 2022; 952-956. https://doi.org/10.1109/ISMSIT56059.2022.9932652 .

21. Naji NAR. Assessment of image quality of cervical spine complications using Three Magnetic Resonance Imaging Sequences. Baghdad Sci J. 2023; 20(3(Suppl.): 1155. https://doi.org/10.21123/bsj.2023.8244.

نهج إحصائي جديد للحصول على أفضل شريحة رؤية في تسلسل الرنين المغناطيسي لأورام الدماغ

حسن الياسين 1، محمد عبد الرحيم فضل 2، عمران الشماع 1

1جامعة تكنولوجيا المعلومات والاتصالات، بغداد، العراق
2كلية علوم الحاسوب وتكنولوجيا المعلومات، جامعة سومر، ذي قار، العراق.

الخلاصة

يعزز تشخيص أورام الدماغ المبكر احتمالات شفاء المرضى. مع تقدم استخدام الذكاء الاصطناعي في مجال الطب، أصبح اكتشاف أورام الدماغ أحد اهتمامات الباحثين. لا تزال مسألة تحديد أي شريحة في تسلسل الرنين المغناطيسي تعطي أفضل رؤية للورم تحديًا. قدم هذا البحث نهجًا إحصائيًا جديدًا لاستخراج الورم من فحص رنين الدماغ للمريض (تسلسل). في البداية، تم حساب دالة الكتلة الاحتمالية (PMF) لكل صورة في التسلسل. ثم تم تطبيق تقنية انحراف كولباك-ليبلر لتحديد الصورة أو الصور التي انحرفت عن الصور الصحية ذات الصلة. تم تحديد أفضل شريحة رؤية للورم باستخدام مقياس جذر متوسط الخطأ. بالإضافة إلى ذلك، تم تطبيق نهج تجميع لتجزئة الصور الورمية. تم استخدام طريقة التجميع الكمي (VQ) لتجميع الصور في 16 مجموعة مختلفة، في حين تم استخدام تقنية VQ عكسية لإنتاج صور ثنائية التنغيم. في النهاية، تم استخدام طريقة Teager ثنائي الأبعاد لاكتشاف الحواف لتحديد الورم. تم استخدام مجموعة بيانات خاصة تتضمن عشرين فحصًا بالرنين المغناطيسي (تسلسلًا) للاختبار وتقييم النظام.

الكلمات المفتاحية: أورام الدماغ، انحراف كولباك-ليبلر ، صور الرنين المغناطيسي، دالة الكتلة الاحتمالية، اكتشاف الأورام.